Polym. Bull. (2012) 69:241–259
DOI 10.1007/s00289-012-0751-9

ORIGINAL PAPER

Rheology, morphology and tensile properties of reactive compatibilized polyethylene/polystyrene blends via Friedel–Crafts alkylation reaction

Kh. Shahbazi · M. K. Razavi Aghjeh · F. Abbasi · M. Partovi Meran · M. Mehrabi Mazidi

Received: 9 November 2011 / Revised: 19 January 2012 / Accepted: 28 March 2012 /
Published online: 7 April 2012

Abstract Attempts were made to study the effect of reactive compatibilization via Friedel–Crafts alkylation reaction, using $AlCl_3$ as a catalyst, on rheology, morphology, and mechanical properties of polyethylene/polystyrene (PE/PS) blends. The results of linear viscoelastic measurements in conjunction with the results of the mixing torque variation indicated that PS showed much more degradation than that of PE in the presence of $AlCl_3$. It was also found that while for PE-rich blends, the viscosity, and storage modulus increased by reactive compatibilization, they decreased for PS-rich blends. The variation of viscosity and storage modulus for 50/50 blend was found to be dependent on frequency ranges showing the competitive effects of PE–*g*–PS copolymer formation and PS degradation. The results of morphological studies showed that reactive compatibilization decreased the particle size and particle-size distribution broadness because of in situ graft copolymer formation. Reactive compatibilization enhanced the tensile strength and elongation at break for PE-rich blends. It was demonstrated that there is a close interrelationship between rheology, morphology, and mechanical properties of reactive compatiblized PE/PS blends. It was also demonstrated that rheological behaviors have a reliable sensitivity to follow the structural and morphological changes during compatibilization process, so that, those information can be used to predict the morphology as well as mechanical properties of the blends.

Keywords Polyethylene · Polystyrene · Compatibilization · Friedel–Crafts alkylation

Kh. Shahbazi · M. K. Razavi Aghjeh (✉) · F. Abbasi · M. Partovi Meran · M. Mehrabi Mazidi
Department of Polymer Engineering, Institute of Polymeric Materials,
Sahand University of Technology, 51335-1996 Sahand New Town, Tabriz, Iran
e-mail: karimrazavi@sut.ac.ir

Introduction

Polyolefins/Polystyrene blends, similar to other immiscible polymer blends, suffer from low interfacial interaction, which results in poor mechanical properties [1–5]. Different compatibilization processes are used to enhance mechanical properties of immiscible polymer blends. These compatibilization processes are based on the improvement of the adhesion between phases and reduction of interfacial tension which lead to a stable morphology [5–7]. The most common method has been used to increase compatibility of the immiscible polymer blends is adding of a block or graft copolymer which contains compatible segments with blend constituents [8–17]. Reactive compatibilization is another interested method from economic and academic points of view in which the compatibilizer is generated during the blending process and preferentially locates at the blend interface. Because neither polyolefins nor polystyrene have any functional group, a number of reactive polymer reagents have been used for the reactive compatibilization of these blends [18–22]. Another possibility for in situ compatibilization of polyolefin/polystyrene blends is an electrophilic substitution of a proton on the aromatic ring of polystyrene by a halogenated alkane or olefin in the presence of a strong Lewis acid; known as Friedel–Crafts (F–C) alkylation reaction [23, 24]. Carrick [25] synthesized a copolymer of PE and PS using $AlCl_3$ as an F–C alkylation reaction catalyst in a solution. Using the same method, Heikens and co-workers [26, 27] prepared a PE–*g*–PS copolymer and then added into PE/PS melt blends and reported improvements in both morphology and mechanical properties. Based on the findings of Baker and co-workers [28, 29] $AlCl_3$ has the highest reaction efficiency among all the studied Lewis acids. Gao et al. [30] used $AlCl_3$ to compatibilize LLDPE/PS and LLDPE/HIPS blends and examined the structure of graft copolymer and confirmed that LLDPE segments were grafted to the para position of the benzene rings of PS. Diaz et al. [31, 32] studied the relation between the molecular weight of the used polyethylene and the structure of the formed graft copolymer and the effect of the architecture and content of graft copolymer on the efficiency of compatibilization process. Although a considerable number of research works has been published on the reactive compatibilization of polyolefin/polystyrene blends via F–C alkylation reaction, there is a few works on the relationships between rheology and morphology of these reactive compatibilized blends. In this study, attempts were made to study the rheology, morphology, and mechanical properties of reactive compatiblized PE/PS blends via F–C alkylation reaction using $AlCl_3$ as a catalyst. The processing characteristics of these blends were also studied as a preliminary step in understanding the role of different parameters on these processes. In this study, a close relationship between the rheology and morphology of the reactive compatibilized blends was demonstrated.

Experimental

Materials

HDPE and PS with specifications summarized in Table 1 both from Tabriz Petrochemical Company, Iran, were used as received. $AlCl_3$ as a catalyst were purchased from Merck.

Table 1 Specifications of the blend constituents

Polymer	MFI (g/10 min)	M_w (g/mol)	PDI
HDPE	4.0 (190 °C, 2.16 kg)	712000	2.29
PS	11.4 (200 °C, 5 kg)	686500	1.76

Sample preparation

The melt compounding of all the blends containing various amounts of PS (25, 50, and 75 wt%) was carried out in a laboratory batch internal mixer (Brabender W50 EHT) at 180 °C with a rotor speed of 60 rpm. The chamber volume was 55 cc and the filling factor was selected 0.8. Therefore, the weights of the different constituents were measured based on their weight ratios in blend and their melt densities. A small amount of each prepared blend was rapidly quenched in liquid nitrogen for morphological studies and the remaining was compression molded into sheets with a thickness of 2 mm in a Dr. Collin (P200P; 25 MPa) laboratory hot press at 180 °C for 5 min under 10 MPa pressure to use in rheometry and tensile tests. Then the sheet samples were cooled within the cast under 10 MPa pressure for 1.5 min.

Rheological studies

Rheological properties of the neat PE, neat PS, un-compatibilized and reactive compatibilized PE/PS blends were investigated using a stress-controlled rheometer (UDS 200, Anton Paar) equipped with parallel plate geometry (diameter = 25 mm, gap = 1 mm). The frequency sweep tests were performed in the range of 0.1–500 rad/s at 180 °C with amplitude of 1 % in order to maintain the response of the materials in the linear viscoelastic regime.

Morphology observation

Morphology of the blends was examined using scanning electron microscopy method (SEM LEO 440 I, UK). Only the cryo-fractured surfaces of the PE-rich blend and 50/50 blend were etched with xylene for 6 h at 50 °C for the removal of PS phase. Then surfaces were gold sputtered for good conductivity of the electron beam and microphotographs were taken with a magnification of ×5,000.

Tensile properties

A Zwick/Roell tensile testing machine (Z 010) was used to carry out the tensile tests for all samples according to ASTM D-638 at crosshead speed of 50 mm/min. At least five trials were performed per each sample and the mean values were reported.

Degree of grafting measurements

The degree of grafting was measured using solvent extraction method followed by FTIR studies. Thin films of the samples were immersed in THF solvent for removal

of un-grafted PS. The samples were dried in a vacuum oven at 80 °C for 12 h for removal of THF solvent. FTIR spectra of different samples were analyzed for measuring the extent of grafted PS using a calibration curve.

Results and discussion

Processing characteristic

Figure 1 shows the variation of the mixing torque of the internal mixer versus time obtained for neat PS and PS in the presence of $AlCl_3$. Dramatically decrease of the mixing torque appeared after $AlCl_3$ addition is due to the chain scission of PS, which leads to its molecular weight (M_w) decrease [30–33]. The variation of the mixing torque versus time obtained for neat PE and PE with $AlCl_3$ are shown in Fig. 2. At first glance one may guess that addition of $AlCl_3$ does not affect the molecular structure of PE. Although in other research works it has been noticed that $AlCl_3$ has not a clear effect on PE structure [30], but decisive discretion may be resulted from rheological measurements applied on these samples (Sect. 'Rheology and Morphology').

Figure 3 indicates the mixing torque–time curve of PE/PS 75/25 blend with and without $AlCl_3$. As it can be seen, after feeding of $AlCl_3$, the mixing torque increases and decreases after passing through a maximum, and then tends to a plateau. By considering the effect of $AlCl_3$ on the mixing torques of neat PE and neat PS (Figs. 1, 2), increasing in mixing torque after $AlCl_3$ feeding observed for PE/PS 75/25 blend can be related to the formation of PE–*g*–PS copolymer near the blend interphase via F–C alkylation reaction. For PE/PS 75/25 blend, where the PE and PS

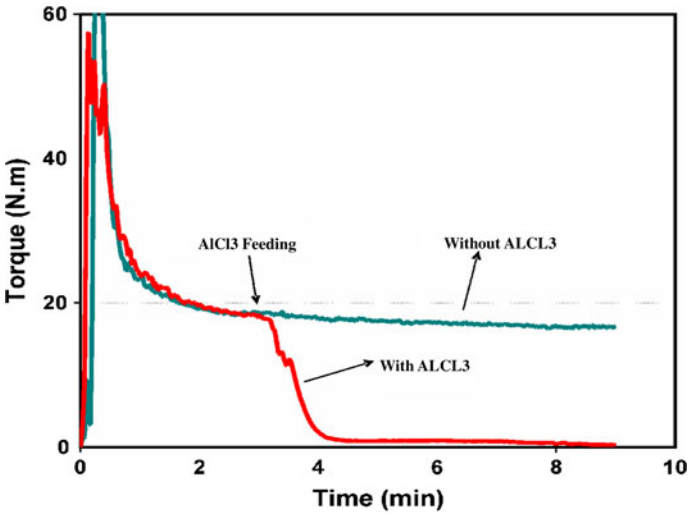

Fig. 1 Variation of the mixing torque of the internal mixer versus time obtained for neat PS and PS in the presence of $AlCl_3$

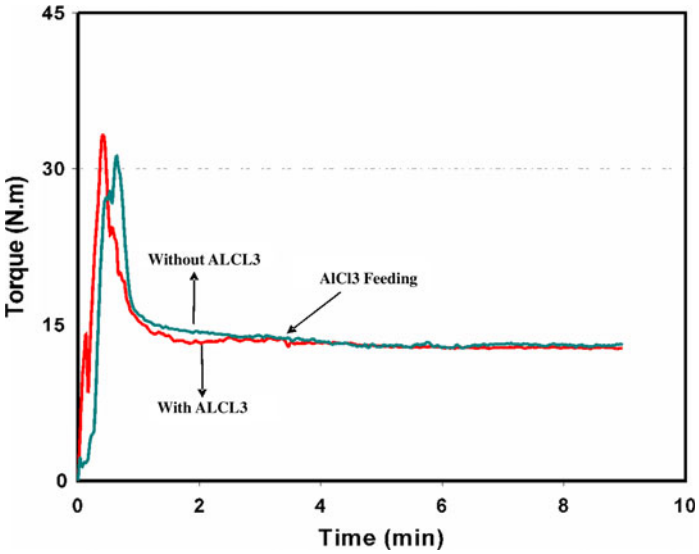

Fig. 2 Variation of the mixing torque of the internal mixer versus time obtained for neat PE and PE in the presence of $AlCl_3$

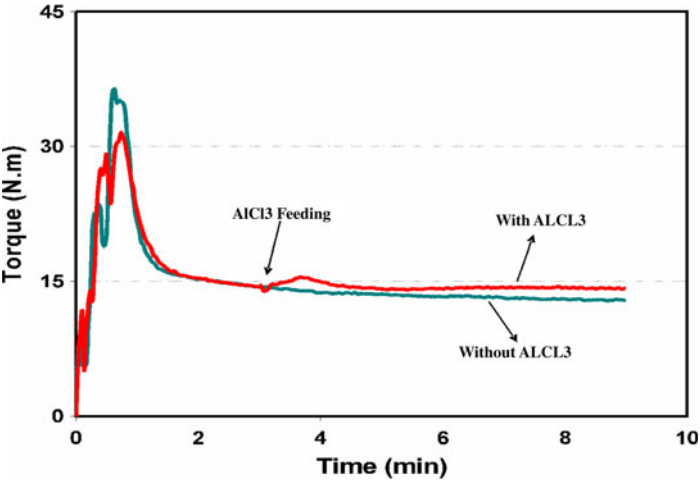

Fig. 3 Variation of the mixing torque of the internal mixer versus time obtained for PE/PS 75/25 with and without of $AlCl_3$

form matrix and dispersed phase, respectively, $AlCl_3$ diffuses in PE phase at first and then reaches to the blend interphase, leading to formation of PE–*g*–PS copolymer. Formation of such a copolymer increases the M_w from one side and reduces the interfacial tension between PE and PS phase from the other side. Increasing in M_w and interfacial interaction can increase the melt viscosity and

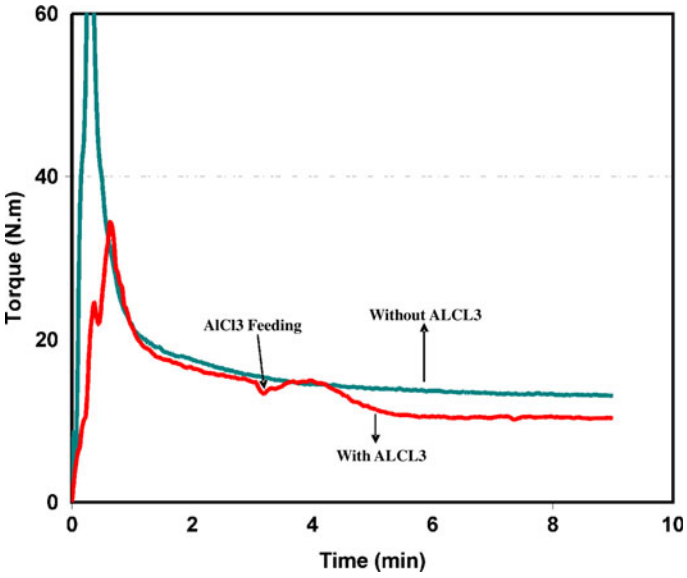

Fig. 4 Variation of the mixing torque of the internal mixer versus time obtained for PE/PS 50/50 with and without of $AlCl_3$

therefore the mixing torque. Decreasing of the mixing torque beyond the maximum is due to the degradation of dispersed PS phase at the later stages of the process.

Effect of $AlCl_3$ on the mixing torque-time curve of 50/50 blend is shown in Fig. 4. As the results show, the variation trend of the mixing torque is similar to 75/25 blend, but with further decrease in mixing torque at the final stages of the process. It will be shown using rheological studies that the used PS has higher viscosity and elasticity than that of the used PE. Therefore, it can be claimed that the PE forms continues phase in PE/PS 50/50 blend. So, the discussion made for 75/25 blend can also be made for 50/50 blend. Moreover, the more decrease in mixing torque at later stages is due to the PS phase degradation.

Figure 5 shows the effect of $AlCl_3$ on the mixing torque of 25/75 blend. As it can clearly be seen, despite of 75/25 and 50/50 blends, the mixing torque decreases dramatically after the $AlCl_3$ addition, then increases and tends to a plateau after passing through a maximum. The difference between the variation trend of the mixing torque for 25/75 blend compared to 75/25 and 50/50 blends can be related to their different morphologies. In 25/75 blend, despite of two other blends, PS and PE form matrix and dispersed phases, respectively. So, at the first stage of reactive compatibilization process, $AlCl_3$ degrades the PS matrix phase and the remaining $AlCl_3$ diffuses toward the blend interphase and leads to PE–*g*–PS copolymer formation. As discussed earlier, the generation of PE–*g*–PS copolymer can increase the melt viscosity and therefore mixing torque. It should be noted that the competitive effects of PS degradation and PE–*g*–PS formation on the later stages of the process, induces a maximum in mixing torque. At the final stages of the process, where the blend interphase is saturated with copolymer, further degradation of PS

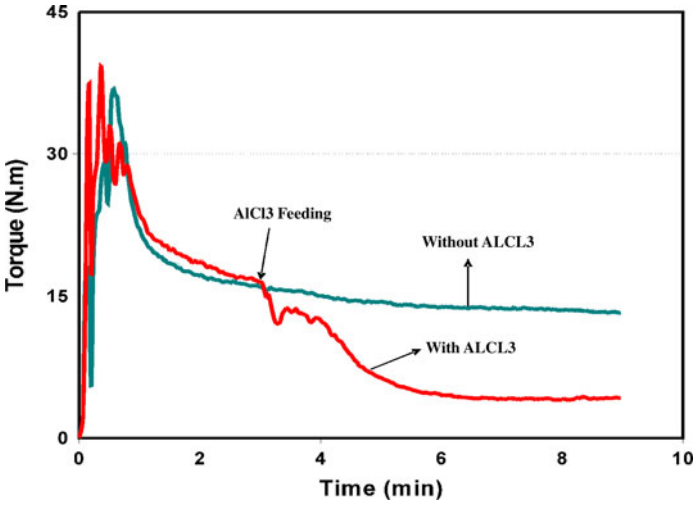

Fig. 5 Variation of the mixing torque of the internal mixer versus time obtained for PE/PS 25/75 with and without of $AlCl_3$

phase causes a more decrease in mixing torque. These results show that only using mixing torque–time curves useful information can be obtained about the reactive compatibilization.

Degree of grafting measurements

Figure 6 shows the results of degree of grafting as a function of PS content. The degree of grafting increases with PS content increase. However, the rate of increasing of the degree of grafting decreases at higher PS contents. These results are in a good agreement with the results of literature [31].

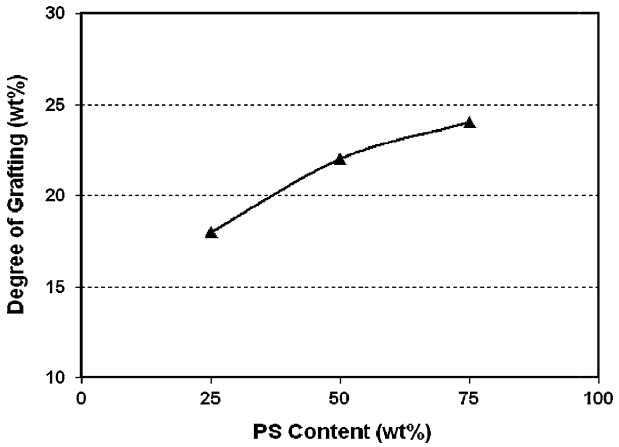

Fig. 6 Variation of the degree of grafting as a function of PS content

Rheology and morphology

The results of complex viscosity (η^*) and storage modulus (G') as functions of angular frequency (ω) obtained for PE and PS are shown in Fig. 7. The results indicate that both PE and PS show a power law type behavior as shear-thinning. On the other hand, as it can be seen, the PS has higher viscosity and elasticity than PE in most ranges of angular frequency. Figures 8 and 9 show the results of complex viscosity and storage modulus versus angular frequency for blend samples having different compositions. These results clearly indicate that similar to the blends' components, PE/PS blends show shear-thinning behavior and almost exhibit an intermediate behavior between PE and PS. It may be thought that addition of 25 % high-viscous PS onto low-viscous PE will increase its viscosity and elasticity. But it is interesting to note that the 25/75 blend has lower viscosity and elasticity compared to neat PE. This can be due to the poor interfacial interaction between PE and PS phases [30].

The results of linear viscoelastic studies, applied in small amplitudes, can provide reliable information on microstructure of the blends. The viscoelastic response of the blends at low frequencies, where the effect of flow-induced molecular orientation on viscosity and elasticity become more less, can be used for evaluating of the interfacial interaction between phases [34–38]. The complex viscosity and storage modulus versus blend composition together with the same results calculated using linear mixing rule at angular frequency of 0.1 rad/s are presented in Figs. 10 and 11, respectively. It can clearly be seen that, the complex viscosity and in particular storage modulus show remarkable negative deviation from mixing rule for all the blends. On the base of Utracki's studies [39, 40], this type of behavior

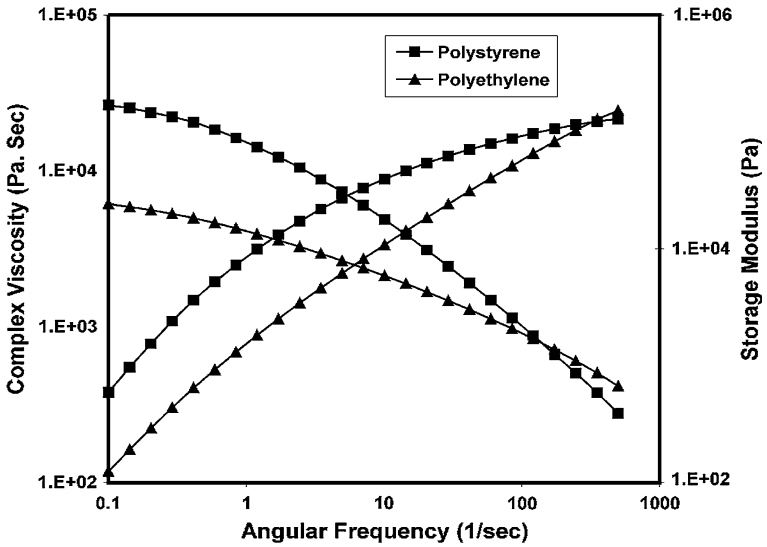

Fig. 7 The results of complex viscosity (η^*) and storage modulus (G') as functions of angular frequency (ω) for PE and PS

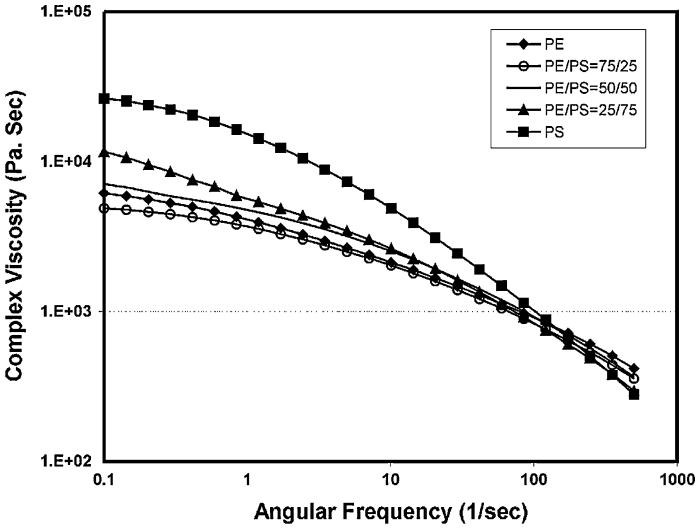

Fig. 8 Complex viscosity versus angular frequency for blend samples having different compositions

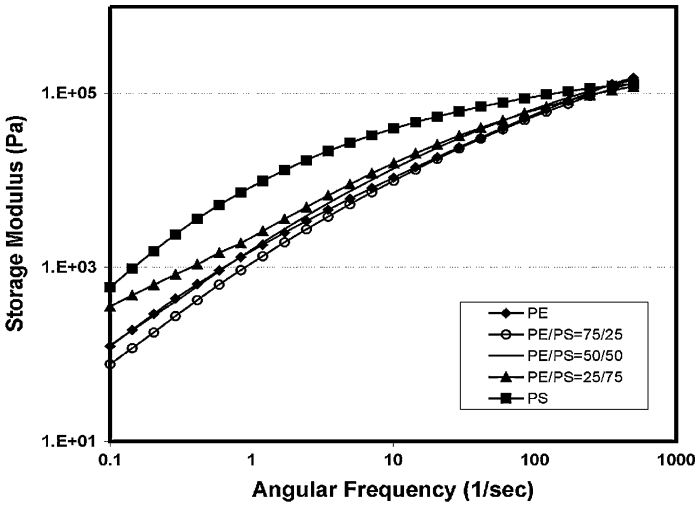

Fig. 9 Storage modulus versus angular frequency for blend samples having different compositions

(negative deviation bond) can be observed in blends with a low interfacial tension. In other words, from these results it can be concluded that all the blends exhibit low interfacial interaction.

Figure 12 shows the complex viscosity and storage modulus versus angular frequency for neat PE and PE processed with $AlCl_3$. These results show that the PE processed with $AlCl_3$ has lower viscosity and elasticity at low frequencies and displays higher viscosity and elasticity at high frequencies compared to neat processed PE. In other words, addition of $AlCl_3$ decreases the shear-thinning

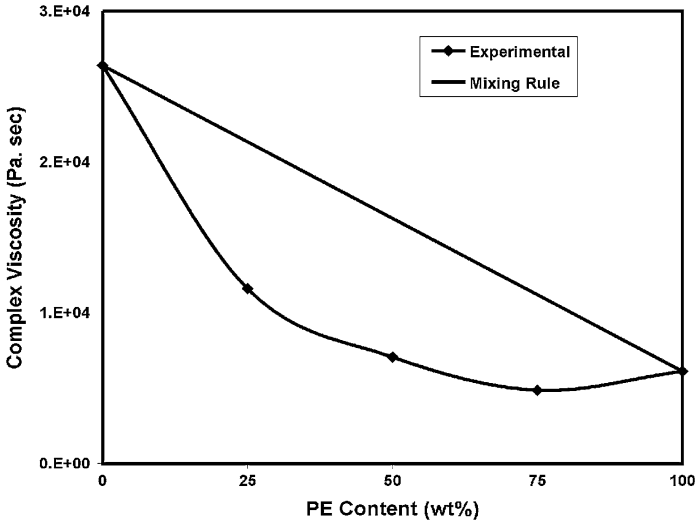

Fig. 10 Complex viscosity versus blend composition together with the same results calculated using linear mixing rule at angular frequency of 0.1 rad/s

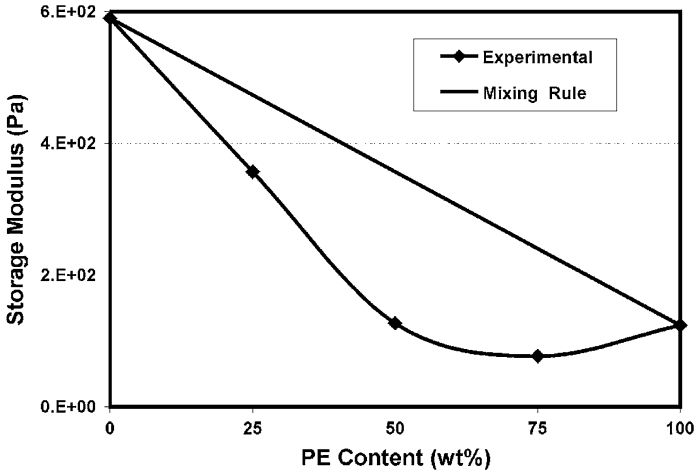

Fig. 11 Storage modulus versus blend composition together with the same results calculated using linear mixing rule at angular frequency of 0.1 rad/s

behavior of the PE. So, it can be resulted that, $AlCl_3$ causes a slight chain scission in PE in particular larger chains leading to decreasing in its molecular weight and molecular weight distribution (M_wD) broadness. Gao and Diaz [30, 31] showed that addition of $AlCl_3$ increases melt flow index of PE.

Figure 13 shows the relaxation time distribution spectrum $H(\lambda) \cdot \lambda$ as a function of relaxation time (λ) for neat PE and PE with $AlCl_3$. There are two points in this figure. The first is that PE has a bimodal relaxation time distribution corresponding

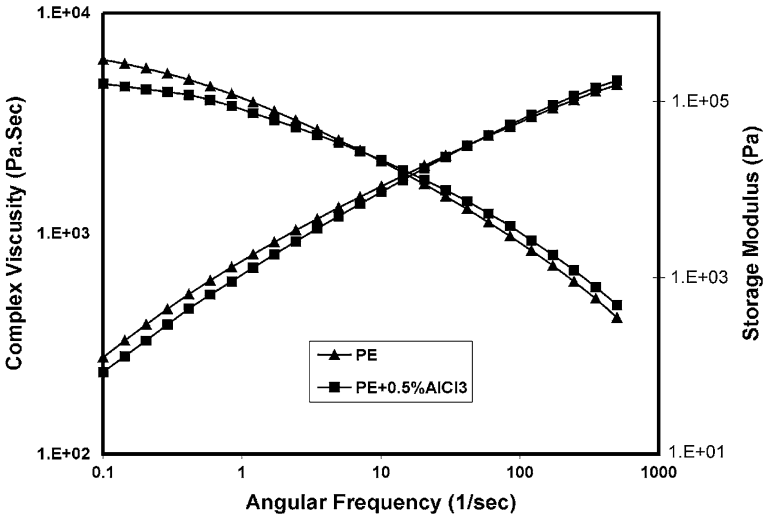

Fig. 12 Complex viscosity and storage modulus versus angular frequency for neat PE and PE processed with $AlCl_3$

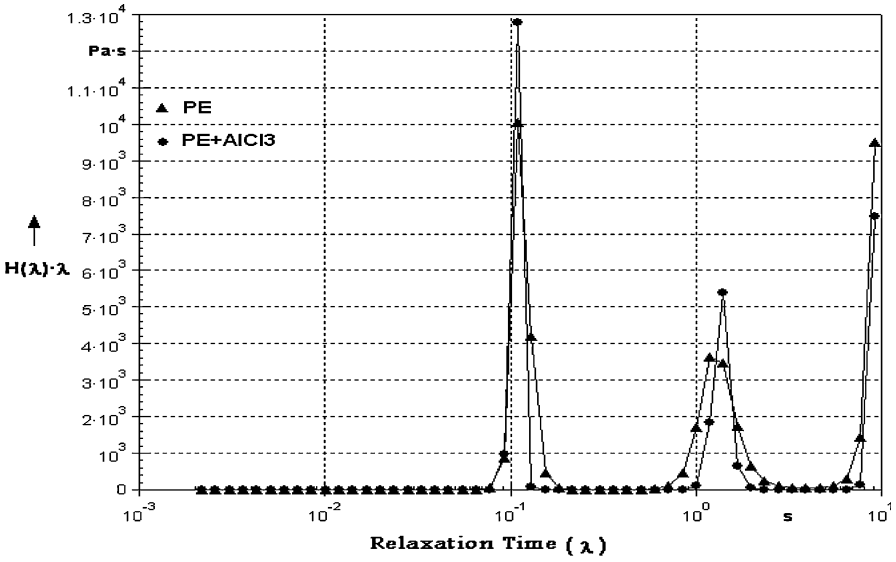

Fig. 13 Relaxation time distribution spectrums, $H(\lambda) \cdot \lambda$, as functions of relaxation time (λ) for neat PE and PE processed with $AlCl_3$

to its bimodal M_wD. The second is that addition of $AlCl_3$ decreases the M_wD on both low and high relaxation time ranges. Figure 14 shows the effect of $AlCl_3$ on the rheological behavior of PS. These results clearly show that addition of $AlCl_3$ dramatically decreases the viscosity and elasticity of PS representative of its severe degradation in the presence of $AlCl_3$.

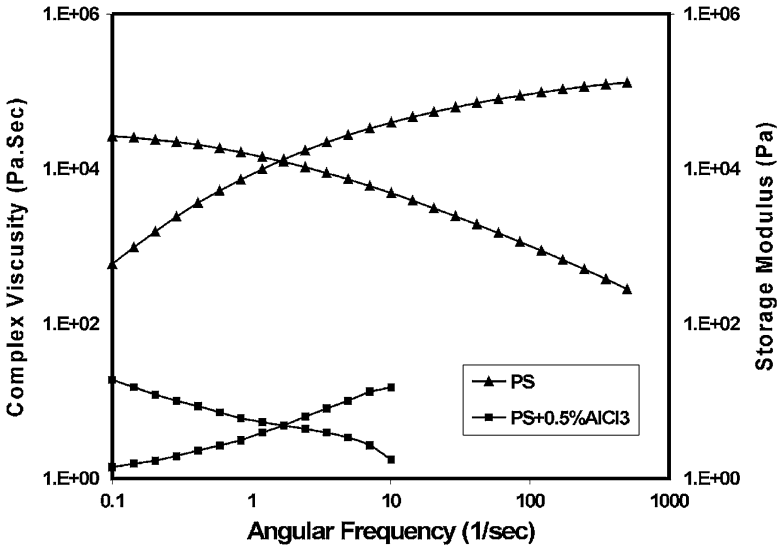

Fig. 14 Complex viscosity and storage modulus versus angular frequency for neat PS and PS processed with $AlCl_3$

Effect of $AlCl_3$ on the rheological behavior of PE/PS 75/25 blends is shown in Fig. 15. Addition of $AlCl_3$ increases the viscosity and elasticity of PE/PS 75/25 blend in all frequency ranges. These results confirm the obtained results using torque–time curves. In other words, in this blend composition, addition of $AlCl_3$ increases the viscosity and elasticity due to the formation of PE–*g*–PS copolymer.

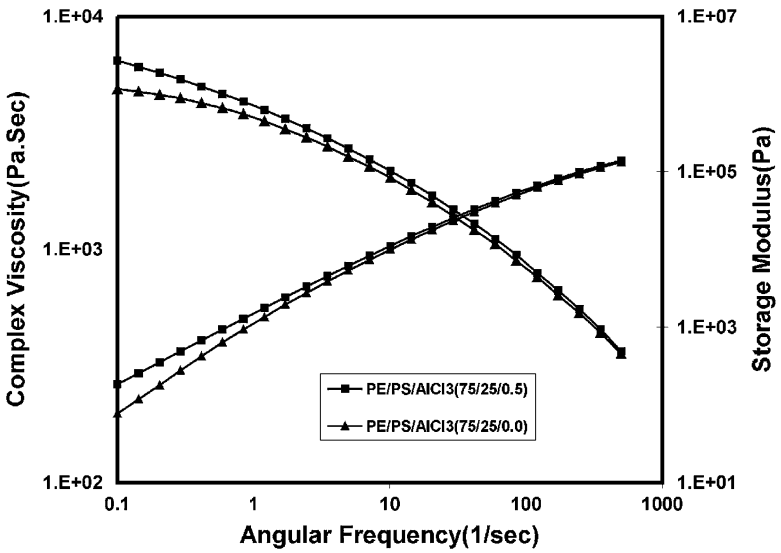

Fig. 15 Effect of $AlCl_3$ on the rheological behavior of PE/PS 75/25 blend

By considering the fact that, in this process both PE and in particular PS phases undergo chain scission leading to decrease in their viscosity and elasticity, such increase in the viscosity and elasticity can be related to the formation of PE–*g*–PS copolymer, which can increase the average M_w of the blend near the interphase and can reduce interfacial tension leading to increase in interfacial interaction. In such reactive compatibilized blends there are three different components including un-grafted PE, un-grafted PS, and PE–*g*–PS copolymer. It has been found that un-grafted PS and un-grafted PE have lower M_w compared to neat PS and PE, respectively [31]. It has also been found that PE–*g*–PS copolymer has a higher M_w compared to the physical blend of PE/PS with the same PE/PS ratio. So, increasing of viscosity and elasticity of PE/PS 75/25 blend is due to the formation of such a copolymer.

The relaxation time distribution spectra of un-compatibilized and reactive compatibilized PE/PS 75/25 blends are shown in Fig. 16. These results clearly show that contrary to PE, addition of $AlCl_3$ increases the relaxation time distribution broadness of this blend. The formation of high-molecular weight PE–*g*–PS copolymer from one side, and degradation of both PS and PE phases from the other side, increases the molecular weight distribution broadness and hence relaxation time distribution broadness. Appearance of tails at lower relaxation times can be related to the relaxation of individual small PE chains pendent to PS main chains.

Figure 17 shows the complex viscosity and storage modulus of un-compatibilized and reactive compatibilized PE/PS 50/50 blends. It is interesting to note that contrary to PE/PS 75/25 blend, in this blend composition addition of $AlCl_3$ increases

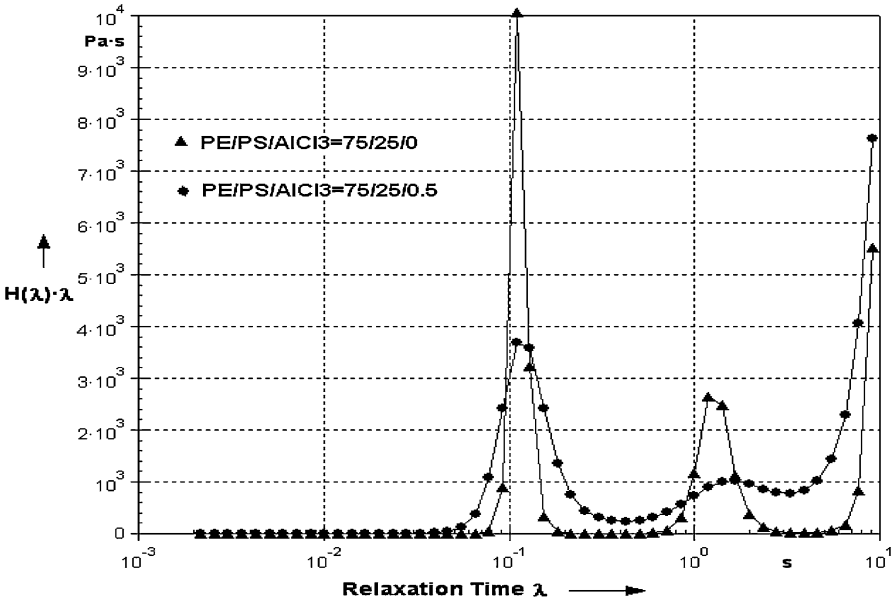

Fig. 16 Relaxation time distribution spectrums of un-compatibilized and reactive compatibilized PE/PS 75/25 blends

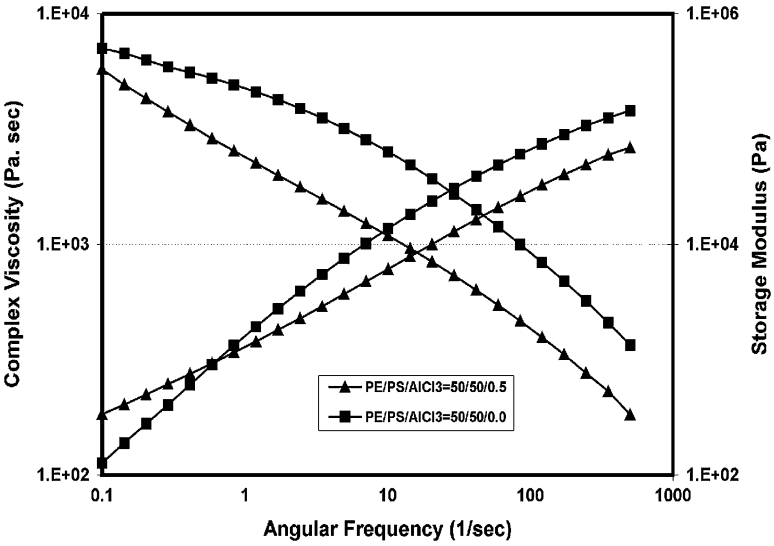

Fig. 17 Complex viscosity and storage modulus of un-compatibilized and reactive compatibilized PE/PS 50/50 blends

the elasticity at low frequencies but decreases it at high frequencies. These results illustrate that due to the higher amount of PS in this blend composition compared to 75/25 blend, the effect of PS degradation predominates the effect of PE–*g*–PS copolymer formation. But at low frequencies, where the effect of molecular orientation on the viscosity and elasticity becomes more less, the effect of PE–*g*–PS copolymer formation on the interfacial interaction is more visible. As the results of the degree of grafting measurements showed, the amount of the formed PE–*g*–PS in this composition is higher than that of 75/25 blend. For this reason, the extent of elasticity increment for 50/50 blend is higher than that of 75/25 blend at low frequencies. The same results for PE/PS 25/75 blend can be seen in Fig. 18. It is clear from these results that $AlCl_3$ causes an obvious decrease in viscosity and elasticity in all frequency ranges. This is due to the further degradation of higher content PS matrix. However, the formation of PE–*g*–PS can be concluded from the low frequency ranges data, where the elasticity tends to a plateau. In this blend composition, the effect of PS degradation is more predominant than the effect of copolymer formation. From the results obtained using rheological studies it can be predicted that reactive compatibilization will increase and decrease the mechanical properties of the PE- and PS-rich blends, respectively.

Morphology observation

Figure 19 shows the SEM micrographs of un-compatibilized and reactive compatibilized PE/PS blends. As it can be seen, un-compatibilized PE/PS 75/25 blend displays a matrix-dispersed morphology. The dispersed PS particles exhibit low interaction to PE matrix leading to formation of a broad size distribution.

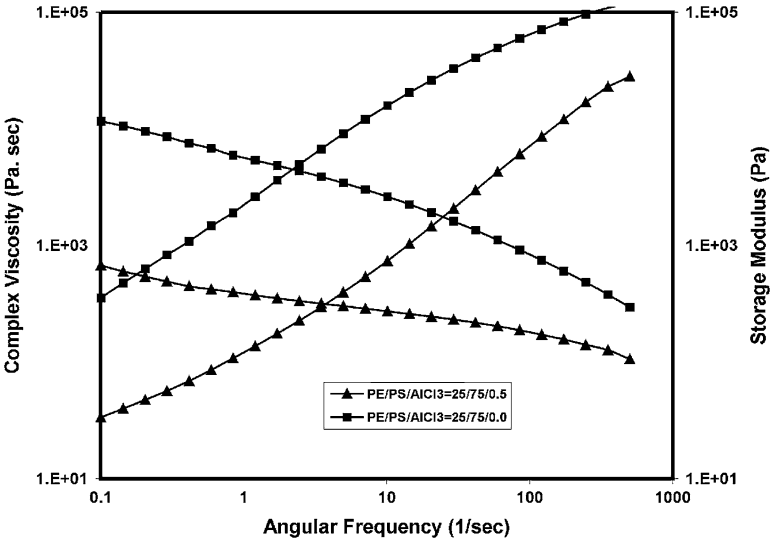

Fig. 18 Complex viscosity and storage modulus of un-compatibilized and reactive compatibilized PE/PS 25/75 blends

The particle size and particle-size distribution have decreased after reactive compatibilization process, due to the formation of PE–*g*–PS copolymer and its localization at the PE/PS interface. Formation of such copolymer increases the interfacial interaction between PE and PS phases leading to effective stress transfer from matrix to dispersed phase and decreases the coalescence of the droplets. Owing to the higher viscosity of PS than that of PE (Fig. 7) PS remains as dispersed phase in PE/PS 50/50 blend but with large domain size and it seems that the composition is near the phase inversion composition. Based on the findings which indicate that PS undergoes much more viscosity decrease than that of PE after $AlCl_3$ addition, it may be predicted that addition of $AlCl_3$ may lead to phase inversion of PE/PS 50/50 blend. The result conversely shows that after $AlCl_3$ addition PS display dispersed phase yet with decrease in domain size. This is due to the fact that before diffusion of $AlCl_3$ onto the PS phase it reaches to the interface and forms the PE–*g*–PS copolymer which can stabilize the morphology. Moreover, the formation of PE–*g*–PS copolymer increases the interfacial interaction and reduces the particle size.

For un-compatibilized PE/PS 25/75 blend, PE is the dispersed phase. Compatibilization has decreased the particle size and increased the interfacial interaction which can be concluded from its fractured surface. During the fracturing process, well-adhered PE particles showed plastic deformation representative of good adhesion between phases.

Tensile properties

The results of mechanical properties showed that reactive compatibilization considerably enhanced the mechanical properties of PE-rich blend. After

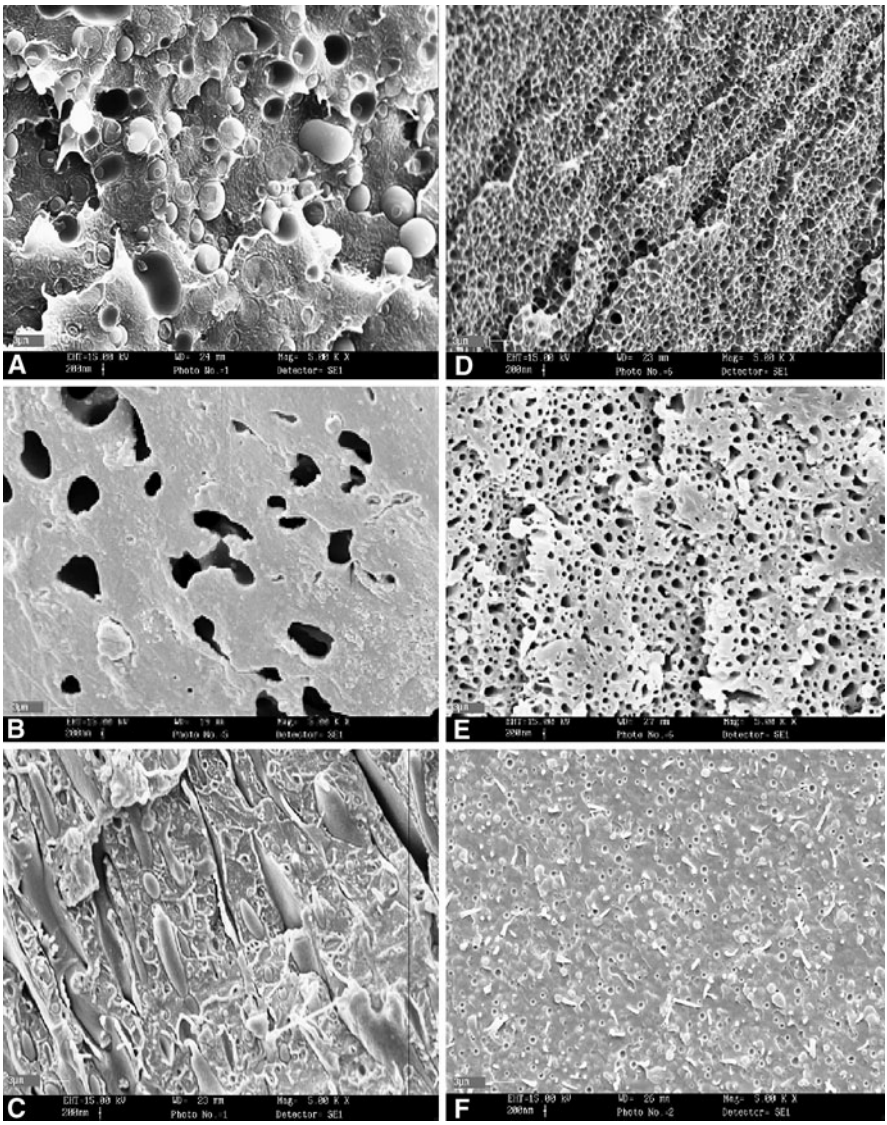

Fig. 19 SEM micrographs of un-compatibilized and reactive compatibilized PE/PS blends. **a** PE/PS75/25, **b** PE/PS50/50, and **c** PE/PS25/75 un-compatibilized. **d** PE/PS75/25, **e** PE/PS50/50, and **f** PE/PS25/75 reactive compatibilized

compatibilization the tensile strength and elongation at break of PE/PS 75/25 blend increased from 9.8 MPa and 240 % to 11.2 MPa and 884 %, respectively. For PE/PS 50/50 blend the extent of mechanical properties increment was as much as PE/PS 75/25 blend. Its elongation at break increased from about 4.2 to 152 %. Although the interface of this blend is also improved during compatibilization process, but severe degradation of PS phase does not allow a higher increase in

mechanical properties. PE/PS 25/75 blend showed decrement in mechanical properties after compatibilization due to the degradation of PS matrix phase. From these results it can be concluded that reactive compatibilization via F–C alkylation reaction is more useful in PE-rich blend but not for PS-rich blends. These results verify the reliability of the predicted results using rheological measurements.

Conclusion

Processing characteristic, rheology, morphology, and mechanical properties of reactive compatibilized PE/PS blends were studied and the obtained results were conducted to the following conclusions:It was found that in the presence of $AlCl_3$ the grafting reaction preferentially occurs at the blend interface. Therefore, transposition of degradation and grafting reactions is strongly affected by the blend morphology and hence by the blend composition. In PE-rich blends, due to the grafting reaction and therefore copolymer generation, the M_w and M_wD broadness increased. While, in PS-rich blends, in spite of copolymer formation the M_w and M_wD broadness decreased in the result of PS phase degradation. During reactive compatibilization process, the interfacial interaction between the matrix and dispersed phases increased due to the formation of PE–*g*–PS copolymer which in turn led to finer and well-distributed particles. Reactive compatibilization increased the mechanical properties of the PE/PS blends in particular for PE-rich blends. The rheological behavior and viscoelastic properties of the blends have a reliable sensitivity for evaluating the interfacial interaction. So, the information obtained from these studies can be used in the prediction of the morphology and therefore mechanical properties of the blends.

References

1. Utracki LA (1998) Commercial polymer blends. Springer, New York
2. Utracki LA (1989) Polymer alloys and blends. Hanser, Munich
3. Bisio AT, Xantos M (1995) How to manage plastics waste: technology and market opportunities. Hanser, Munich
4. Utracki LA (1991) Two-phase polymer systems. Hanser, Munich
5. Wu S (1982) Polymer interfaces and adhesion. Marcel Dekker, New York
6. Milner S, Xi H (1996) How copolymers promote mixing of immiscible homopolymers. J Rheol 40:663–687
7. Favis BD (2000) Factors influencing the morphology of immiscible polymer blends in melt processing. In: Paul DR, Bucknall CB (eds) Polymer blends, vol 1. Wiley, New York, pp 501–535
8. Fayt R, Jerome R, Teyssie P (1982) Molecular design of multicomponent polymer systems. III: Comparative behavior of pure and tapered block copolymers in emulsification of blends of low-density polyethylene and polystyrene. J Polym Sci 20:2209–2217
9. Fayt R, Jerome R, Teyssie P (1982) Molecular design of multicomponent polymer systems XIV: control of the mechanical properties of polyethylene–polystyrene blends by block copolymers. J Polym Sci 27:775–793
10. Fayt R, Jerome R, Teyssie P (1987) Characterization and control of interfaces in emulsified incompatible polymer blends. Polym Eng Sci 27:328–334

11. Utracki LA, Sammut P (1990) On the uniaxial extensional flow of polystyrene/polyethylene blends. Polym Eng Sci 30:1019–1026
12. Lindsay CR, Paul DR, Barlow JW (1981) Mechanical properties of HDPE–PS–SEBS blends. J Appl Polym Sci 26:1–8
13. Schwarz MC, Keskkula H, Barlow JW, Paul DR (1988) Deformation behavior of HDPE/(PEC/PS)/SEBS blends. J Appl Polym Sci 35:653–677
14. Guo HF, Packirisamy S, Mani RS, Aronson CL, Gvozdic NV, Meier DJ (1998) Compatibilizing effects of block copolymers in low-density polyethylene/polystyrene blends. Polymer 39:2495–2505
15. Xu SA, Tjong SC (2000) Deformation mechanisms and fracture toughness of polystyrene/high-density polyethylene blends compatibilized by triblock copolymer. J Appl Polym Sci 77:2024–2033
16. Macaubas PHP, Demarquette NR (2001) Morphologies and interfacial tensions of immiscible polypropylene/polystyrene blends modified with triblock copolymers. Polymer 42:2543–2554
17. Jianming L, Ma PL, Favis BD (2002) The role of the blend interface type on morphology in Co-continuous polymer blends. Macromolecules 35:2005–2016
18. Simmons A, Baker W (1989) Basic functionalization of polyethylene in the melt. Polym Eng Sci 29:1117–1123
19. Baker W, Saleem M (1987) Polystyrene-polyethylene melt blends obtained through reactive mixing process. Polym Eng Sci 27:1634–1641
20. Liu N, Baker W, Russell K (1990) Functionalization of polyethylenes and their use in reactive blending. J Appl Polym Sci 41:2285–2300
21. Sun Y, Flaris V, Baker W (1997) Evaluation and characterization of vector fluids and peroxides in a process of in situ compatibilization of polyethylene and polystyrene. The Can J Chem Eng 75:1153–1158
22. Lagardere P, Baker W (1998) Mechanical properties and morphology of copolymer modified polymer blends. Polymer 56:198–202
23. Morrison R. T, Boyd R. N (1973) Electrophilic Aromatic Substitution. In: Organic Chemistry, Allyn and Bacon, New York, pp 337-371
24. Reinhard B (2002) Substitution reactions on aromatic compounds. In: Advanced organic chemistry, Harcourt/Academic Press, San Diego, pp 169–217
25. Carrick WL (1970) Reactions of polyolefins with strong lewis acids. J Polym Sci A 8:215–223
26. Barentsen WM, Heikens D (1973) Mechanical properties of polystyrene/low density polyethylene blends. Polymer 14:579–583
27. Heikens D, Barentsen W (1977) Particle dimensions in polystyrene/polyethylene blends as a function of their melt viscosity and of the concentration of added graft copolymer. Polymer 18:69–72
28. Sun Y, Baker WE (1997) Polyolefin/polystyrene in situ compatibilization using Friedel–Crafts alkylation. J Appl Polym Sci 65:1385–1393
29. Sun Y, Willemse RJG, Liu TM, Baker WE (1998) In situ compatibilization of polyolefin and polystyrene using Friedel–Crafts alkylation through reactive extrusion. Polymer 39:2201–2208
30. Gao Y, Huang H, Yao Z, Shi D, Ke Z, Yin J (2003) Morphology, structure, and properties of in situ compatibilized linear low-density polyethylene/polystyrene and linear low-density polyethylene/high-impact polystyrene blends. J Polym Sci B 41:1837–1849
31. Diaz MF, Barbosa SE, Capiati NJ (2002) Polyethylene–polystyrene grafting reaction: effects of polyethylene molecular weight. Polymer 43:4851–4858
32. Diaz MF, Barbosa SE, Capiati NJ (2007) Reactive compatibilization of PE/PS blends: effect of copolymer chain length on interfacial adhesion and mechanical behavior. Polymer 48:1058–1065
33. Pukanszky B, Kennedy JP, Kelen T, Tudos F (1981) Cationic reactions in the melt 1. The effect of Lewis acids on polystyrene. Polym Bull 5:469–476
34. Graebling D, Benkira A, Gallot Y, Muller R (1994) Dynamic viscoelastic behaviour of polymer blends in the melt—experimental results for PDMS/POE-DO, PS/PMMA and PS/PEMA blends. Eur Polym J 30:301–308
35. Germain Y, Ernest B, Genelot O, Dhamani L (1994) Rheological and morphological analysis of compatibilized polypropylene/polyamide blends. J Rheol 38:681–697
36. Graebling D, Muller R, Palierne JF (1993) Linear viscoelastic behavior of some incompatible polymer blends in the melt, interpretation of data with a model of emulsion of viscoelastic liquids. Macromolecules 26:320–329
37. Gramespacher H, Meissner J (1992) Interfacial tension between polymer melts measured by shear oscillations of their blends. J Rheol 36:1127–1141

38. Lacroix C, Grmela M, Carreau PJ (1998) Relationships between rheology and morphology for immiscible molten blends of polypropylene and ethylene copolymers under shear flow. J Rheol 42:41–62
39. Utracki LA (1991) On the viscosity-concentration dependence of immiscible polymer blends. J Rheol 35:1615–1638
40. Jorgensen L, Utracki L (1991) Dual phase continuity in polymer blends. Makromol Chem, Macromol Symp 48–49:189–209